

# Synthesis and Characterization of Poly(*o*-Toluidine) Doped with Organic Sulfonic Acid by Solid-State Polymerization

Tursun Abdiryim, Zhang Xiao-Gang, Ruxangul Jamal

School of Chemistry and Chemical Engineering, Xinjiang University, Urumqi 830046, China

Received 20 April 2004; accepted 23 September 2004

DOI 10.1002/app.21614

Published online in Wiley InterScience (www.interscience.wiley.com).

**ABSTRACT:** Poly(*o*-toluidine) (POT) salts doped with organic sulfonic acids ( $\beta$ -naphthalene sulfonic acid, camphor sulfonic acid, and *p*-toluene sulfonic acid) were directly synthesized by using a new solid-state polymerization method. The FTIR spectra, ultraviolet visibility (UV-vis) absorption spectra, and X-ray diffraction patterns were used to characterize the molecular structures of the POT salts. Voltammetric study was done to investigate the electrochemical behaviors of all these POT salts. The FTIR and UV-vis absorption spectra revealed that the POT salts were composed of mixed oxidation state phases. All POT salts contained the conducting emeraldine salt (half-oxidized and protonated form)

phase; the pernigraniline (fully oxidized form) phase is predominant in POT doped with  $\beta$ -naphthalene sulfonic acid, and POT doped with *p*-toluene sulfonic acid had the highest doping level. The X-ray diffraction patterns showed that the obtained POT doped with organic sulfonic acids were lower at crystallinity. The conductivity of the POT salts were found to be of the order  $10^{-3}$ – $10^{-4}$  S/cm. © 2005 Wiley Periodicals, Inc. *J Appl Polym Sci* 96: 1630–1634, 2005

**Key words:** conducting polymer; poly(*o*-toluidine); synthesis; solid-state polymerization; organic sulfonic acids

## INTRODUCTION

Polyaniline (PANi) is one of the most interesting conducting polymers because of its environmental stability, ease in preparation, exciting electrochemical, optical, and electrical properties, and possible applications in rechargeable batteries, microelectronics devices, biosensors, electrochromic displays, and chemical sensors.<sup>1–7</sup> However, the main disadvantages of this polymer are its insolubility in common organic solvents and its infusibility. Alternative methods have been designed to improve the solubility and processibility of the PANi and its synthesized derivatives. It was found that ring-substituted (alkyl and alkoxy) and *N*-alkyl-substituted PANi are more soluble than unsubstituted PANi.<sup>8</sup>

Therefore, many studies have been devoted to the synthesis of soluble PANi derivatives.<sup>9–11</sup> Poly(*o*-toluidine) (POT) is similar to PANi; thus, being an example of this important family of conducting polymers, it can be synthesized either chemically or electrochemi-

cally as a bulk powder or film.<sup>11</sup> POT occurs in four different oxidation states (Figure 1); only emeraldine salt is the conducting form of POT.

Recently, PANi doped with  $\beta$ -naphthalene sulfonic acid and camphor sulfonic acid were successfully synthesized by solid-state polymerization method.<sup>12</sup> In this article, the POT doped with organic sulfonic acids (e.g.,  $\beta$ -naphthalene sulfonic acid, camphor sulfonic acid, and *p*-toluene sulfonic acid) were synthesized by the solid-state polymerization method and the resulted POT salts were examined by the FTIR spectra, ultraviolet visibility (UV-vis) absorption spectra, and X-ray diffraction patterns. Their electrochemical behavior was also studied.

## EXPERIMENTAL

### Synthesis

*o*-Toluidine (analytical reagent, AR; Xi'an Chemical Reagent Co., China) monomer was distilled under reduced pressure. Other reagents, such as dopants ( $\beta$ -naphthalene sulfonic acid, camphor sulfonic acid, and *p*-toluene sulfonic acid; AR, Acros Organics) and oxidants (ammonium peroxydisulfate, APS; AR, Xi'an Chemical Reagent Co., Xi'an, China), were used as received.

A typical solid-state polymerization procedure was followed<sup>12</sup>: 1 mL distilled water and 2.08 g  $\beta$ -naphthalene sulfonic acid (NSA) were put in the mortar; they were ground to dissolve the acid (as much as possi-

Correspondence to: Z. Xiao-Gang (azhangxg@163.com).

Contract grant sponsor: National Natural Science Foundation of China; contract grant number: 20403014.

Contract grant sponsor: Xibu Zhiguang Science Foundation of China.

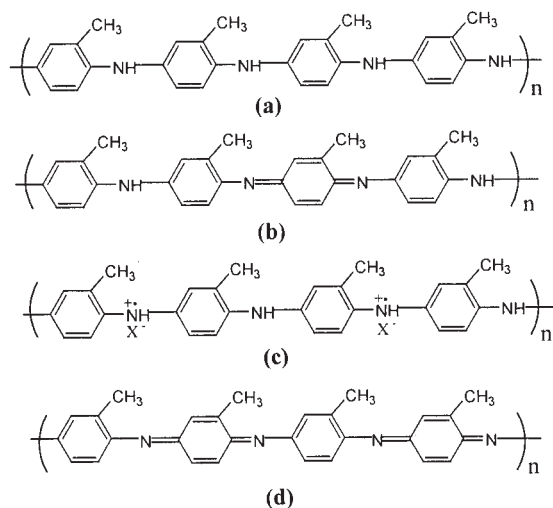


**Figure 1** Four different redox forms of POT: (a) leucoemeraldine base (fully reduced form), (b) emeraldine base (half-oxidized form), (c) conducting emeraldine salt (half-oxidized and protonated form), (d) pernigraniline base (fully oxidized form).

ble), and then freshly distilled 1 mL *o*-toluidine was added drop-wise. After grinding the reactant  $\sim$  10 min, the mixture became a white paste, and 2.2 g APS was added by further grinding for 20 min until the color of the solid changed to black-green. The greenish-black powder was washed with ethyl ether, ethanol, and distilled water, respectively, until the filtrate was colorless; then, the powder was dried under vacuum at 50°C for 48 h.

POT salts with camphor sulfonic acid (POT-CSA) and *p*-toluene sulfonic acid (POT-*p*-TSA) as dopant were synthesized in a similar manner.

### Characterization

FTIR spectra of the polymers were obtained by using a Bruker Equinox-55 Fourier transform infrared spectrometer (Billerica, MA) (frequency range, 3500–400  $\text{cm}^{-1}$ ). UV-vis spectra of the polymer solution in *m*-cresol were recorded by using a Hitachi-U3010 double-beam spectrophotometer (Tokyo, Japan) in the range of 300–900 nm. The X-ray diffraction studies were performed on a D/Max 2400 X-ray diffractometer (Tokyo, Japan) by using  $\text{CuK}\alpha$  radiation source ( $\lambda = 0.15418$  nm). The scan range ( $2\theta$ ) was 10°–70°. The room temperature conductivity was measured on pressed pellets with a diameter of 1 cm by using a two-probe technique. Electrochemical measurements were carried out with a classical three-electrode cell by using a CHI660A electrochemical workstation system (Cordova, TN). The working electrode was a POT film electrode prepared by casting the DMF solution of respective POT salts on a platinum electrode. The reference electrode was Ag/AgCl, and the counter-

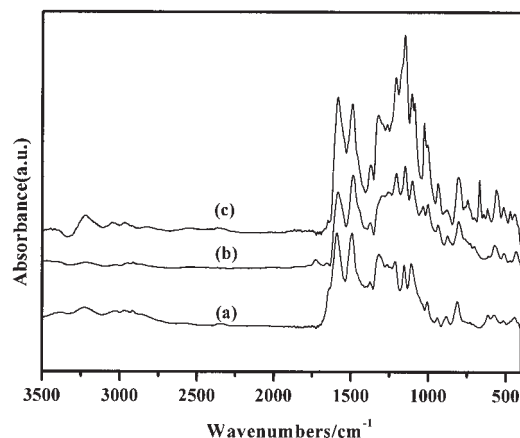


**Figure 2** FTIR spectra of (a) POT-*p*-TSA, (b) POT-CSA, and (c) POT-NSA.

electrode was a 1- $\text{cm}^2$ -area Pt flag. Inherent viscosities ( $\eta_i$ ) were determined at 25°C on freshly prepared solutions of POT salts (0.1%) in concentrated sulfuric acid by using a Ubbelohde viscometer. A 0.1% POT salt solution was prepared by stirring polymer powder in concentrated sulfuric acid for 6 h.

## RESULTS AND DISCUSSION

### IR spectra

Figure 2 showed the FTIR spectra of POT salts synthesized by solid-state synthesis method; the band assignments are summarized in Table I. The characteristic bands at  $\sim$  2915–2917  $\text{cm}^{-1}$  can be assigned to the stretching vibration of the methyl ( $-\text{CH}_3$ ) group.

**TABLE I**  
Band Wavenumber and Assignments of the POT Salts

Band position ( $\text{cm}^{-1}$ )			Assignment <sup>a</sup>
POT-NSA	POT-CSA	POT- <i>p</i> -TSA	
565	577	569	$\nu\text{S}=\text{O}$
809	807	812	$\gamma\text{CH}$
880	877	882	$\gamma\text{CH}$
940	939	941	$\gamma\text{CH}(\text{Q})$
1004	1003	1005	$\delta\text{CH}$ , $\nu\text{S}=\text{O}$
1028	1034	1028	$\gamma\text{C}-\text{CH}_3$ , $\nu\text{S}=\text{O}$
1108	1104	1110	$\delta\text{CH}$
1152	1150	1155	$\delta\text{CH}$
1210	1207	1213	$\nu\text{CN}$ , $\delta\text{CH}$
1324	—	1318	$\nu\text{CN}$
1374	1376	1375	$\delta\text{CH}_3$
1490	1487	1492	$\nu\text{CC}$
1586	1585	1591	$\nu\text{CC} + \nu\text{QN}$
—	1728	—	$\nu\text{C}=\text{O}$
2916	2915	2917	$\nu\text{CH}_3$
3221	—	3229	$\nu\text{NH}_2^+$ , $\text{NH}^+$ , $\nu\text{NH}$

<sup>a</sup> Q denotes quinoid units of the polymers;  $\nu$ : stretching mode;  $\delta$ : bending mode;  $\gamma$ : deformation mode.

**TABLE II**  
Relative Intensity of Quinoid to Benzenoid Ringmodes of the POT Salts

Sample	$I_{\sim 1585-1591}/I_{\sim 1487-1492}$
POT-NSA	1.1
POT-CSA	0.82
POT- <i>p</i> -TSA	1.0

The two bands appearing at  $\sim 1585-1591 \text{ cm}^{-1}$  and  $\sim 1487-1492 \text{ cm}^{-1}$  correspond to the stretching vibration of the quinoid and benzenoid ring, respectively. The bands at  $\sim 1374-1375 \text{ cm}^{-1}$  are due to the symmetric deformation of methyl group. The bands at  $\sim 1318-1324$  and  $\sim 1207-1213 \text{ cm}^{-1}$  can be assigned to the C—N mode, whereas the bands at  $\sim 1150-1155$ ,  $\sim 1104-1110$ , and  $\sim 1003-1005 \text{ cm}^{-1}$  are the characteristic bands of C—H vibration.<sup>13-16</sup> The three bands appearing at  $\sim 807-812$ ,  $\sim 877-882$ , and  $\sim 939-941 \text{ cm}^{-1}$  were attributed to an out-of-plane C—H vibration, 1,2,4-substitution in the benzenoid rings, and an in-plane C—H vibration of quinoid rings.<sup>16</sup> The presence of the  $-\text{SO}_3$  group is confirmed by the appearance of bands around  $\sim 565-577$ ,  $\sim 1003-1005$ , and  $\sim 1028-1034 \text{ cm}^{-1}$  in all spectra of POT salts.<sup>15,17</sup> The presence of the vibration band of the dopant ion and other characteristic bands confirm that the POT salts contain the conducting emeraldine salt phase.

The presence of bands at  $\sim 1585-1591$  and  $\sim 1487-1492 \text{ cm}^{-1}$  clearly shows that the polymer is composed of amine and imine units. Further, it gives support to an earlier prediction of the presence of different oxidation states of the polymer. The relative intensities of these bands point toward the oxidation state of the polymer.<sup>18</sup> The relative intensity of quinoid-to-benzenoid ring modes ( $I_{\sim 1585-1591}/I_{\sim 1487-1492}$ ) was 1.0, 0.82, and 1.1 for POT-*p*-TSA, POT-CSA, and POT-NSA, respectively (Table II).

A value of 1.0 defines the emeraldine-type structure and the polymer can have higher conductivity; increasing the oxidation level of the polymer to  $>1.0$  would result in a decrease in conductivity.<sup>18c</sup> A comparison of the ratio of the relative intensity of quinoid-to-benzenoid ring modes ( $I_{\sim 1585-1591}/I_{\sim 1487-1492}$ ) shows the highest ratio of 1.1 in POT-NSA compared to POT-*p*-TSA and POT-CSA. From the above results, it can be concluded that the formation of the fully oxidized pernigraniline phase is predominant in POT-NSA.

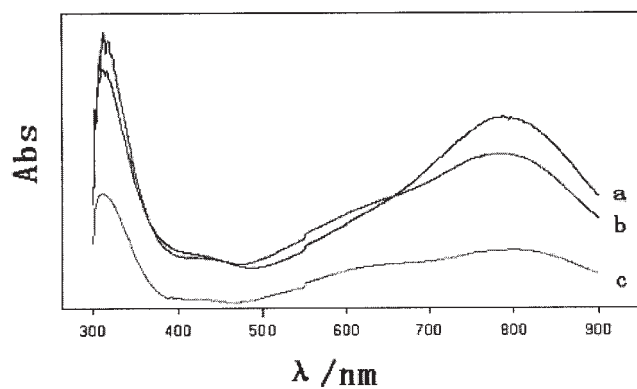
### UV-vis spectra

Figure 3 represented the UV-vis absorption spectra of POT salts in *m*-cresol solution. These POT salts show three characteristic absorption peaks at 312–318, 414–417, and 785–800 nm, whereas one more shoulder

appears at 645 nm in the spectrum of POT-NSA (Figure 3). The absorption peak at  $\sim 312-318 \text{ nm}$  can be ascribed to  $\pi-\pi^*$  transition of the benzenoid rings, whereas the peaks at 414–417 and 785–800 nm can be attributed to polaron- $\pi^*$  transition and  $\pi$ -polaron transition, respectively.<sup>15,19,20</sup> The shoulder at 645 nm appearing in the spectrum of POT-NSA can be assigned to the exciton transition resulting from electron transfer from benzenoid to quinoid rings.<sup>21</sup> Based on the previous research that the extent of doping can be roughly estimated from the absorption spectra of the polyaniline, in which the ratio of absorbances at 785–800 and 312–318 nm indicated the doping level of polyaniline,<sup>21,22</sup> it was found that, in the case of POT salts, the intensity ratio ( $A_{785-800}/A_{312-314}$ ) was smallest in POT-CSA, which meant that the doping level of POT-CSA was lower than 2 that of POT-*p*-TSA and POT-NSA.

### XRD analysis

Crystallinity and orientation of conducting polymers have been of much interest, because more highly ordered systems can display a metallic-like conductive state.<sup>23</sup> Jozefowicz et al. made the detailed and systematic study on the POT prepared by the conventional methods and proposed a pseudo-orthorhombic unit cell structure for POT.<sup>24</sup> The X-ray diffraction patterns for the POT salts were shown in Figure 4. X-ray diffraction patterns showed that the POT salts have low crystallinity with broad diffraction peaks, but the Bragg diffraction peaks of  $2\theta \sim 8^\circ, 15^\circ, 20^\circ$ , and  $25^\circ$  with low intensity can be found in the X-ray patterns in the POT-*p*-TSA and POT-CSA; however, POT-NSA appears almost amorphous. This is due to the doping level of POT that crystallinity of POT increases with the doping level; such an effect, which can be explained by the fact that the insertion of doping anions between polymer chains makes the polymer structure more rigid, favors the crystalline state.<sup>24</sup>



**Figure 3** UV-vis spectra of (a) POT-*p*-TSA, (b) POT-CSA, and (c) POT-NSA.

TABLE III  
The Assignments of UV-Vis Absorption Peaks of POT Salts

Polymer	Wavelength of absorption peak				$A_{785-800}/A_{312-318}$
	$\pi-\pi^*$ transition (nm)	Polaron- $\pi^*$ transition (nm)	Exciton transition (nm)	$\pi$ -polaron transition (nm)	
POT-NSA	312	417	645	800	0.65
POT-CSA	318	414	—	785	0.61
POT- <i>p</i> -TSA	314	415	—	789	0.80

Compared to POT-CSA, the lower crystallinity POT-NSA with the higher doping level may be attributed to the higher ratio of the relative intensities of the quinoid-to-benzenoid ring modes in POT-NSA, which cause the polymer chain to be more compact and less in order.<sup>25</sup>

### Cyclic voltammogram

The redox properties of the POT salts were investigated by using cyclic voltammetry. Figure 5 showed the cyclic voltammograms (CVs) of the polymer films on Pt in 1 mol/L  $H_2SO_4$ . Two redox couples are observed in the CVs of POT-*p*-TSA, POT-CSA, and POT-NSA. The first redox peak (at  $\sim 0.15$ – $0.30$  V) is attributed to the leucoemeraldine-emeraldine transition, whereas the second redox couple (at  $\sim 0.53$ – $0.60$  V) is attributed to the emeraldine-*pernigraniline* transition.<sup>19</sup> Similar cyclic voltammograms were observed with electrochemically and chemically synthesized POT.<sup>26</sup> Compared with the POT-*p*-TSA, the positive shifts in the first redox peak potential of POT-NSA and the negative shifts in the first redox peak potential of POT-CSA were observed. The positive and negative shifts in the first redox potentials of the POT salts can be explained by FTIR results. In the relative intensity of quinoid-to-benzenoid ring modes, the order is POT-

NSA > POT-*p*-TSA > POT-CSA. On the contrary, the electron-withdrawing ability of the quinoid unit is stronger than that of the benzenoid unit in the polymer chain; this led to the first redox potential shifts to higher potential in POT-NSA and lower potential shifts in POT-CSA.<sup>27</sup>

### Conductivity, inherent viscosity

The conductivity, inherent viscosity, and yield of POT salts obtained by solid-state polymerization are listed in Table III. The conductivity of POT salts is about three orders of magnitude less than PANi. Generally, conducting polymers with substituents on their frameworks showed lower conductivities compared with those of the original PANi. Leclerc et al. proposed that the presence of bulky substituents in the polymer chain can induce some nonplanar conformations that decrease the conjugation along the backbone.<sup>28a</sup> The methyl group on the phenyl ring in the POT can be expected to increase the torsional angle between adjacent rings to relieve steric strain and then lead to the lower conductivities of the POT as compared to unsubstituted PANi.<sup>28b</sup> The conductivity of POT synthesized in *p*-TSA is the highest and that synthesized in CSA is the lowest among the POT salts (Table IV); this is in

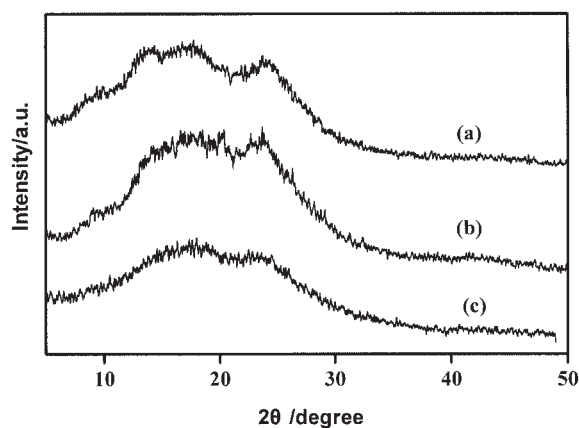


Figure 4 XRD patterns of (a) POT-*p*-TSA, (b) POT-CSA, and (c) POT-NSA.

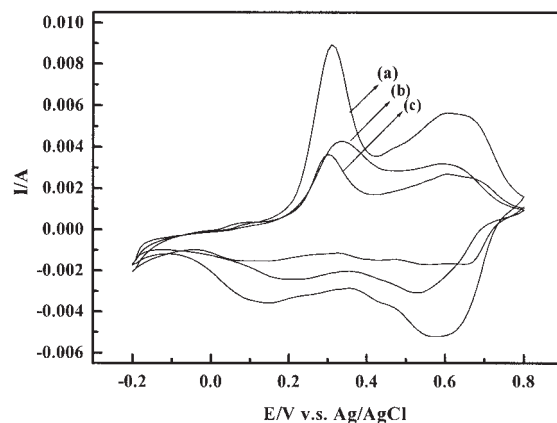


Figure 5 Cyclic voltammograms of (a) POT-*p*-TSA, (b) POT-NSA, and (c) POT-CSA, in 1 mol/L  $H_2SO_4$  solution scan rate: 50 mV/s.

TABLE IV  
The Detailed data of POT salts

Polymer	Conductivity (S/cm)	Yield (%)	Color	$\eta_i$ (dL/g)
POT-NSA	$0.75 \times 10^{-3}$	66	Dark blue	0.18
POT-CSA	$0.62 \times 10^{-3}$	61	Dark blue	0.23
POT- <i>p</i> -TSA	$3 \times 10^{-3}$	51	Blue	0.16

good agreement with the results of FTIR spectra, UV-vis spectra, and CV curves.

The inherent viscosity of the POT salts (Table IV) is low, which is also in good agreement with the observation by previous researchers<sup>8,29</sup> that it is more difficult to obtain high molecular weight of substituted PANi, which means that the inherent viscosity of substituted PANi is lower than that of the parent PANi prepared under identical polymerization conditions.

### CONCLUSION

POT salts doped with organic sulfonic acids (e.g., NSA, CSA, and *p*-TSA) were directly synthesized by using a new solid-state polymerization method. Spectroscopic studies showed the highest ratio of the relative intensities of the quinoid-to-benzenoid unit in NSA-doped POT, whereas the conducting emeraldine salt phase is formed predominantly in *p*-TSA-doped POT and the doping level of POT-CSA is the lowest among the POT salts. These results were further supported by conductivity measurements and cyclic voltammetry. More crystalline POT salt was obtained by doping with *p*-TSA. Among all these organic acids, *p*-TSA was found to be more suitable as a protonic acid medium to attain a POT with high conductivity in this solid-state polymerization method.

### References

- MacDiarmid, A. G.; Chiang, J. C.; Richter, A. F.; Epstein, A. J. *Synth Met* 1987, 18, 285.
- Geniès, E. M.; Boyle, A.; Lapkowski, M.; Tsintavis, C. *Synth Met* 1990, 36, 139.
- MacDiarmid, A. G.; Chiang, J. C.; Halpern, M.; Huang, W. S.; Mu, S. L.; Somasiri, M. L. D.; Wu, W.; Yaniger, S. I. *Mol Cryst Liq Cryst Sci Technol, Sect B* 1985, 121, 73.
- Novak, P.; Muller, K.; Santhanam, K. S. V.; Haas, O. *Chem Rev* 1997, 97, 207.
- Paul, E. W.; Ricco, J. A.; Wrighton, M. S. *J Phys Chem* 1985, 89, 1441.
- Sangodkar, H.; Sukeerthi, S.; Srinivasa, R. S.; Lal, R.; Contractor, A. Q. *Anal Chem* 1996, 68, 779.
- Sukeerthi, S.; Contractor, A. Q. *Anal Chem* 1999, 71, 2231.
- D'Aprano, G.; Leclerc, M.; Zotti, G. *Macromolecules* 1992, 25, 2145.
- (a) Wang, S. L.; Wang, F. S.; Ge, X. H. *Synth Met* 1986, 16, 99. (b) Leclerc, M.; Guay, J.; Dao, L. H. *Macromolecules* 1989, 22, 649. (c) Wei, Y.; Jaag, G. W.; Chan, C. C. F.; Hsueh, K.; Hariharan, R. A.; Patel, S. K.; Whitecar, C. *J Phys Chem* 1990, 94, 7716.
- Lacroix, J. C.; Garcia, P.; Audière, J. P.; Clément, R.; Kahn, O. *Synth Met* 1991, 44, 117. (b) Gupta, M. C.; Umare, S. S. *Macromolecules* 1992, 25, 138.
- Wei, Y.; Focke, W. W.; Wnek, G. E.; Ray, A.; MacDiarmid, A. G. *J Phys Chem* 1989, 93, 495.
- (a) Tursun, A.; Zhang, X. G. *Acta Polym Sin* 2003, 6, 858. (b) Tursun, A.; Zhang, X. G. *Chinese J Appl Chem* 2003, 20, 1099.
- Andrade, E. M.; Molina, F. V.; Florit, M. I. *J Electroanal Chem* 1996, 419, 15.
- Hasik, M.; Drelinkiewicz, A.; Wenda, E.; Paluszkiwicz, C.; Quillard, S. *J Mol Struct* 2001, 596, 89.
- Milind, V. K.; Annamraju, K. V. *Eur Polym Mater* 2004, 40, 379.
- Fujita, I.; Ishiguchi, M.; Shiota, H.; Danj, T.; Kosai, K. *J Appl Polym Sci* 1992, 44, 987.
- (a) Rabolt, J. F.; Clarke, T. C.; Street, G. B. *J Chem Phys* 1979, 71, 4614. (b) Swapna, R. P.; Subrahmanya, S.; Sathyanarayana, D. N. *Synth Met* 2002, 128, 311.
- (a) Furukawa, Y.; Ueda, F.; Hyodo, Y.; Harada, I. *Macromolecules* 1988, 21, 297. (b) Cataldo, F.; Maltese, P. *Eur Polym Mater* 2002, 38, 1791. (c) Huang, L. M.; Wen, T. C.; Gopalan, A. *Mater Lett* 2003, 57, 1765.
- Kumar, D. *Eur Polym J* 2001, 37, 1721.
- Jiang, H.; Geng, Y.; Li, J.; Wang, F. *Synth Met* 1997, 84, 125.
- Athawale, A.; Kulkarni, M. V.; Chabukswar, V. V. *Mater Chem Phys* 2002, 73, 106.
- Xia, H. S.; Wang, Q. *J Nanoparticles Res* 2001, 3, 401.
- Li, Q.; Cruz, L.; Philips, P. *Phys Rev B* 1993, 47, 1840.
- Jozefowicz, M. E.; Epstein, A. J.; Pouget, J. P.; Masters, J. G.; Ray, A.; MacDiarmid, A. G. *Macromolecules* 1991, 24, 5863.
- Douglas, C.; Joel, D. B.; Jing, L.; Jiří, J.; Mira, J.; *Chem Mater* 1995, 7, 1510.
- Andrade, E. M.; Molina, F. V.; Florit, M. I.; Posadas, J. *Electroanal Chem* 1996, 415, 153.
- Hsu, C. H.; Epstein, A. J. *Synth Met* 1997, 84, 51.